Journal of GeoEngineering, Vol. 14, No. 1, pp. 31-39, March 2019
http://dx.doi.org/10.6310/jog.201903_14(1).4

ANALYTICAL SOLUTION FOR PASSIVE EARTH PRESSURE OF *c*-ϕ SOIL USING PRINCIPAL STRESS ROTATION ASSUMPTION

Kourosh Ghaffari Irdmoosa [1] and Hadi Shahir [2*]

ABSTRACT

In the current study, an analytical method was developed for passive earth pressure distribution in c-ϕ soils using the assumption of principal stress rotation. The trajectory of principal stresses was assumed more general than the previous studies and accordingly a general analytical solution including the surcharge and soil cohesion effects was presented which works well in all ranges of parameters. The proposed equation produces a non-linear distribution for the passive earth pressure which is approximately identical to the Rankine pressure at shallow depths and increases sharply near the wall base and becomes larger than the Coulomb's pressure. The passive force and its height of application were obtained less than those of the Coulomb's equation. This indicates that using the Coulomb's passive equation to check the overturning and sliding of retaining walls is not in the safe side.

Key words: Passive pressure, principal stress rotation, *c*-ϕ soil, surcharge, analytical solution.

1. INTRODUCTION

Active and passive earth pressures acting on a rigid retaining wall are conventionally calculated using either Coulomb's or Rankine's theory with a linear distribution. However, the results of experimental studies such as Tsagareli (1965), Fang and Ishibashi (1986), Tang (1988), and Fang *et al.* (1994) have shown that the distribution of the active and passive pressure behind a retaining wall with a rough face is nonlinear. Various wall movement modes, *i.e.*, translation, rotation about base, and rotation about top, were considered in the mentioned studies. In the experimental studies by Rowe and Peaker (1965), Fang *et al.* (2002), and Dou *et al.* (2017), the passive earth pressure was investigated for translational mode of wall movement.

Handy (1985) found that the non-linear distribution of soil pressure is resulted from the soil-wall friction effect which causes principal stress rotation in the backfill soil. Owing to the frictional resistance of the rough wall, the direction of minor and major principal stresses behind the wall change. He assumed that the minor principal stresses on a flat element behind the wall act along a concave arch with a catenary shape and proposed an analytical solution for active earth pressure. Following the Handy's approach, Harrop-Williams (1989), Paik and Salgado (2003), Goel and Patra (2008), Li and Wang (2014), Rao *et al.* (2016), Xie and Leshchinsky (2016), Zhou *et al.* (2016), and Khosravi *et al.* (2016) developed analytical solutions for active earth pressure in various circumstances.

Although non-linear distribution of active earth pressure has been studied by several investigators, a few studies were undertaken on the passive earth pressure. The passive earth pressure distribution for *c*-ϕ soils in translational mode of wall movement was studied by Cai *et al.* (2017). They considered the angle of the principal stress plane at the wall face and at the slip surface to be equal, which led to a novel equation for inclination of the passive slip surface. This equation calculates the slope of the slip surface greater than $\pi/4 - \phi/2$; however, Poncelet (1840) using Coulomb's limit equilibrium approach for the case where wall friction is present, obtained the slip surface inclination less than $\pi/4 - \phi/2$ in the passive condition. Furthermore, when the wall friction become closer to its maximum value ($\delta = \phi$), the model of Cai *et al.* (2017) does not give proper results and the slip surface orientates towards the vertical direction which is a shortcoming of their formulation. Also, the equation proposed by Cai *et al.* (2017) predicts extraordinary large values of passive earth pressure at the wall base. Pain *et al.* (2017) used pseudo-static approach and attained an equation for seismic passive earth pressure of coarse-grained soils in translational mode of wall movement. Assessing the equation of Pain *et al.* (2017) in the static condition for a vertical back face wall, indicates that it has the same weaknesses of the Cai *et al.* (2017) equation and moreover, for a wall without surcharge, it predicts non-zero pressure values at shallow depths which is negative for the wall height more than 1 m and positive for wall height less than 1 m.

Some valuable experimental works have been conducted by Rowe and Peaker (1965); James and Bransby (1970) and Fang *et al.* (2002), which studied the passive earth pressure for translational, rotational and translational modes of wall movement, respectively.

In the present study, a general trajectory of principal stresses was considered and shortcomings of the previous studies were modified which resulted to a general analytical solution for passive earth pressure of *c*-ϕ soils that works well in all ranges of parameters. Both friction and adhesion for the soil-wall interface and surcharge loading on the backfill were considered. In the proposed equation, the slip surface inclination was one of the parameters and its proper value was determined through the parametric analysis.

Manuscript received April 12, 2018; revised August 27, 2018; accepted October 15, 2018.
[1] Ph.D. candidate, Department of Civil Engineering, Faculty of Engineering, Kharazmi University, Tehran, Iran.
[2*] Assistant Professor (corresponding author), Department of Civil Engineering, Faculty of Engineering, Kharazmi University, Tehran, Iran (e-mail: shahir@khu.ac.ir).

2. THE PROPOSED EQUATIONS

2.1 Trajectory of Principal Stresses

In the past studies, various assumptions have been considered for the trajectory of principal stresses such as circle, parabolic, and catenary. In this study, it was found that the parabolic shape for the trajectory of principal stresses is simplifying the equations in the Cartesian coordinates and gives appropriate results. There is not a clear relationship between the shapes of principal stress trajectory and the mode of wall movement in the literature and this can be a good subject for further investigation.

As mentioned, in the current study, the trajectory of the principal stresses was assumed to be parabolic (Fig. 1). A parabolic trajectory has no fixed center of curvature in the polar system. Thus, it is convenient to use Cartesian coordinates. Accordingly, in a horizontal flat element with a θ_w inclination of major principal stresses at the wall an θ_s at the slip surface, it is assumed that the variation of the inclinations of principal stresses in between is linear, so any arbitrary inclination in x coordination (θ_x) is a linear combination of inclinations at the ends (θ_w, θ_s):

$$\theta_x = \left(1 - \frac{x}{B_z}\right)\theta_w + \left(\frac{x}{B_z}\right)\theta_s \tag{1}$$

where θ_x is the angle of the minor principal stress with respect to the horizontal line, θ_w and θ_s are the values of this angle at the wall and slip surface, respectively (Fig. 1), x is the horizontal distance of each point from the wall and B_z is the length of the element at depth z, which equals $(H - z)$ cot α, where α is the angle of the slip surface with respect to the horizon.

There is not a clear relationship between the shapes of principal stress trajectory and the mode of wall movement in the literature and this can be a good subject for further investigation.

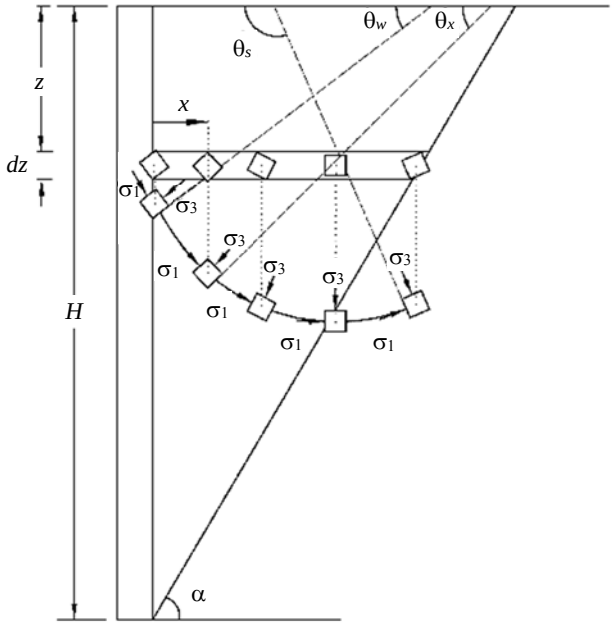

Fig. 1 Trajectory of principal stresses for the passive condition

2.2 Shape of Slip Surface

Coulomb's (1776) assumed that the slip surface at the passive state is a plane at an angle of $\pi/4 - \phi/2$ to the horizon. This angle for the slip surface is predominantly used in practice and gives relatively good results. In the current study, the slip surface was assumed to be planar, but its inclination was considered variable in order to examine its appropriate value. The result of verification analysis presented in the next section, indicated that the slip surface inclination proposed by Coulomb, gives the best approximation to the experimental measurements. Thus, in this study, the slip surface inclination proposed by Coulomb, was adopted which is independent of the soil-wall friction angle. However, it should be noted that the effect of soil-wall friction angle was considered in the other parts of the formulation, which are presented in the following.

2.3 Angle of Principal Stresses

As shown in Fig. 2, the stress state at the wall surface was drawn in the upper half of the Mohr circle where the normal and shear stresses are σ_{hw} and τ_w, respectively, and θ_w is the inclination angle of the principal stress. Both friction and adhesion resistance were considered in the soil-wall interface. The soil-wall friction angle and cohesion are denoted as δ and c_w in Fig. 2, respectively. The stress state at the slip surface was plotted in the lower half of the Mohr circle, which shows the stresses and related angles. In accordance with Fig. 2, the inclination angle of the principal stresses at the wall surface can be obtained as:

$$\theta_w = \frac{\pi}{2} - \frac{1}{2}\sin^{-1}\left(\frac{\sin\delta}{\sin\phi} - \frac{c\cot\phi - c_w\cot\delta}{\sigma_1 - \sigma_3}\sin\delta\right) - \frac{1}{2}\delta \tag{2}$$

As observed, the inclination angle of the principal stresses at the wall surface depends upon the principal stress difference, which varies according to depth. This makes the analytical solution almost impossible to derive. The only assumption which simplifies the above equation and can be applied in the course of the analytical solution is $c_w = c$ (tan δ/tan ϕ), which produces a constant inclination angle as follows:

$$\theta_w = \frac{\pi}{2} - \frac{1}{2}\sin^{-1}\left(\frac{\sin\delta}{\sin\phi}\right) - \frac{1}{2}\delta \tag{3}$$

The inclination angle of the principal stresses at the slip surface (θ_s) according to Fig. 3 is as follows. Note that the angle of slip surface with principal plane is $\pi/4 - \phi/2$.

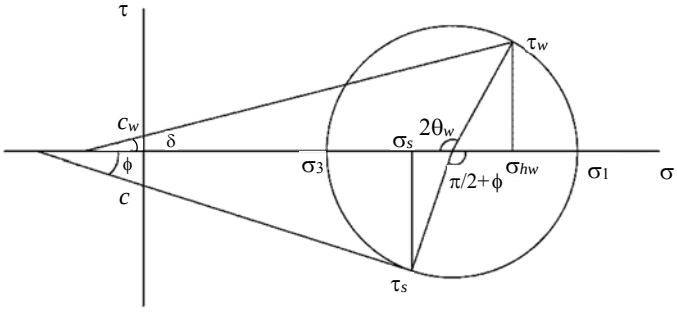

Fig. 2 Mohr circle of stresses at the wall surface and slip surface

$$\theta_s = \alpha + \left(\frac{\pi}{4} + \frac{\phi}{2}\right) \tag{4}$$

where α is the angle of the slip surface with respect to the horizon.

As mentioned, the inclination angle of the principal stress between the wall and the slip surface is assumed to change linearly according to Eq. (1); thus, using Eqs. (1), (3), and (4), the inclination angle of the principal stresses at each point becomes known.

2.4 Stress in Soil Elements

The horizontal and vertical stresses acting on a soil element behind a wall can be expressed versus the principal stress as:

$$\sigma_h = \sigma_1 \sin^2 \theta_x + \sigma_3 \cos^2 \theta_x \tag{5}$$

$$\sigma_v = \sigma_1 \cos^2 \theta_x + \sigma_3 \sin^2 \theta_x \tag{6}$$

According to the Mohr-Coulomb's failure criterion, the relationship between the major and minor principal stresses can be written as:

$$\sigma_1 = K_p \sigma_3 + 2c\sqrt{K_p} \tag{7}$$

where $K_p = \tan^2(\pi/4 + \phi/2)$. The average vertical stress at each level can be obtained by averaging the vertical stresses of the elements between the wall and the slip surface as:

$$\bar{\sigma}_v = \frac{1}{B_z}\int_0^{B_z} \sigma_v \, dx = \frac{1}{B_z}\int_0^{B_z} (\sigma_1 \cos^2 \theta_x + \sigma_3 \sin^2 \theta_x)\, dx \tag{8}$$

where B_z is the distance between the wall and the slip surface at depth z and equals $(H - z)$ cot α. Solving the above integral obtains the following equation for the average vertical stress at each depth:

$$\bar{\sigma}_v = \sigma_1 - (\sigma_1 - \sigma_3)\left[\frac{1}{2} - \frac{\sin 2\theta_s - \sin 2\theta_w}{4(\theta_s - \theta_w)}\right] \tag{9}$$

Substituting the parameters θ_w, θ_s and σ_1 from Eqs. (3), (4) and (7) into Eq. (8) produces the average vertical stress at each depth versus σ_3 at that depth.

2.5 Differential Equation of Equilibrium

Figure 3 shows the differential element of the backfill soil and the stresses acting on it. Using the vertical equilibrium equation for the element, the following differential equation can be obtained. Note that the triangular element shown in Fig. 3 at the right edge of the differential element is in equilibrium; therefore, the normal and shear stresses at the slip surface can be replaced by the major principal stress in the principal plane at which the shear stress is zero.

$$d\,\bar{\sigma}_v B_Z - (\sigma_{hw} \tan\delta + c_w)dz + \sigma_1 \cot\theta_s \, dz = \gamma B_z \, dz \tag{10}$$

where σ_{hw} is the horizontal stress in an element just behind the wall or, in other words, the passive lateral earth pressure on the wall. γ is the unit weight of the backfill soil.

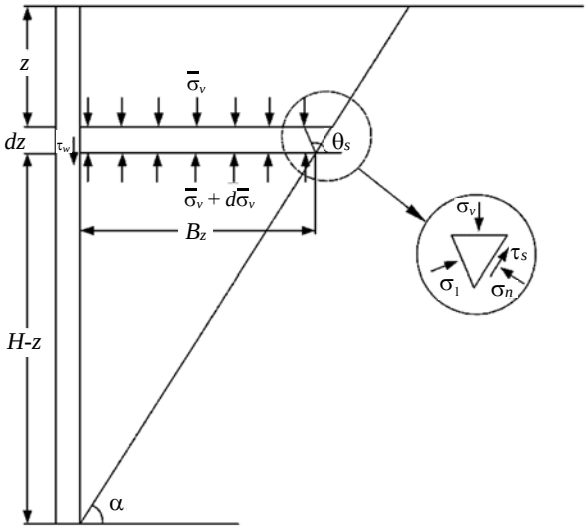

Fig. 3 Free body diagram of differential flat element

By replacing θ_w in Eq. (5), σ_{hw} can be obtained versus the principal stresses. As mentioned above, $\bar{\sigma}_v$ can also be expressed versus σ_3. Consequently, by replacing σ_{hw} and $\bar{\sigma}_v$ versus σ_3 in Eq. (10) and using the chain rule, the following differential equation can be obtained:

$$\frac{d\sigma_3}{dz} = B + \frac{D\sigma_3 + E}{H - z} \tag{11}$$

where H is the height of the retaining wall and z is the depth. Parameters B, D and E are defined as:

$$A = \frac{1}{2} - \frac{\sin 2\theta_s - \sin 2\theta_w}{4(\theta_s - \theta_w)} \tag{12}$$

$$B = \frac{\gamma}{K_p - (K_p - 1)A} \tag{13}$$

$$D = \frac{(K_p \sin^2 \theta_w + \cos^2 \theta_w)\tan\delta - K_p \cot\theta_s}{[K_p - (K_p - 1)A]\cot\alpha} \tag{14}$$

$$E = \frac{2c\sqrt{K_p}(\sin^2 \theta_w \tan\delta - \cot\theta_s) + c_w}{[K_p - (K_p - 1)A]\cot\alpha} \tag{15}$$

Solving Eq. (11) by applying boundary condition $\bar{\sigma}_v = q$ at $z = 0$ obtains σ_3 at each depth as follows:

$$\sigma_3 = F\left(\frac{H}{H - z}\right)^D - \frac{B}{D + 1}(H - z) - \frac{E}{D} \tag{16}$$

where

$$F = \frac{BH}{D + 1} + \frac{E}{D} + \frac{q - 2c\sqrt{K_p}\cos^2 \theta_w}{K_p \cos^2 \theta_w + \sin^2 \theta_w} \tag{17}$$

At back of the wall ($x = 0$), Eq. (5) becomes:

$$\sigma_{hw} = \sigma_1 \sin^2 \theta_w + \sigma_3 \cos^2 \theta_w \quad (18)$$

Now, substituting Eqs. (3), (7), and (16) into the horizontal stress in Eq. (18) obtains the final relationship for the horizontal component of the lateral passive pressure on the rigid retaining wall.

As noticed above, the formulation of this study are based on the following assumptions:

- linear slip surface with angle of $\pi/4 - \phi/2$;
- parabolic shape for trajectory of principal stresses;
- horizontal backfill soil surface and vertical wall back;
- soil-wall adhesion equal to $c_w = c$ (tan δ/tan ϕ).

2.6 Magnitude and Application Point of Passive Earth Pressure

The magnitude of the passive force acting on the rigid retaining wall can be obtained by integrating the passive earth pressure into the height of the wall as:

$$P = \int_0^H \sigma_{hw}\, dz = (K_p \sin^2 \theta_w + \cos^2 \theta_w)\left[\left(\frac{F}{1-D} - \frac{E}{D}\right)H - \frac{BH^2}{2(D+1)}\right] + 2cH\sqrt{K_p}\sin^2 \theta_w \quad (19)$$

The moment of the lateral passive pressure about the wall base can be obtained as:

$$M = \int_0^H \sigma_{hw}(H-z)dz = (K_p \sin^2 \theta_w + \cos^2 \theta_w)\left[\left(\frac{F}{2-D} - \frac{E}{2D}\right)H^2 - \frac{BH^3}{3(D+1)}\right] + cH^2\sqrt{K_p}\sin^2 \theta_w \quad (20)$$

The height of application point of passive force can be obtained by:

$$h = M / P \quad (21)$$

3. VERIFICATION Of THE PROPOSED EQUATION

3.1 Distribution of Lateral Passive Pressure

The results of the proposed equation were verified using the experimental measurements of Fang *et al.* (2002) and Dou *et al.* (2017). In both of these studies, the translational movement was considered.

The experiment of Fang *et al.* (2002) include a 0.5 m wall with backfill unit weight of 16.8 kN/m^3 and ϕ and δ values of 42.1° and 14°, respectively. Dou *et al.* (2017) studied a rigid retaining wall with 1 m height and sand backfill of three different densities. Loose sand with unit weight of 14.21 kN/m^3 and ϕ = 32.6°, medium dense sand with unit weight of 15.64 kN/m^3 and ϕ = 34° and dense sand with unit weight of 16.17 kN/m^3 and ϕ = 43.0°, respectively.

Figure 4 shows the verification results for Fang *et al.* (2002) experiment. As seen, the proposed model has a good approximation comparing to the experimental results. It can be observed that the distribution of the passive pressure in depth is nonlinear and the linear distribution of the soil pressure which is assumed in the Coulomb's theory does not exactly match the actual soil pressure distribution. The passive earth pressure at top of the wall is less than the Coulomb's pressure and is approximately matching with the Rankine pressure. Below the middle of the wall, the rising rate of passive pressure starts to increase gradually and becomes greater than the Rankine's results. Near the wall base, the passive pressure increases sharply and becomes larger than the Coulomb's pressure. This distribution indicates that the Coulomb's equation predicts large values for the passive earth pressure than reality and using this equation for the retaining wall design is not in the safe side.

In Fig. 4, the results of the proposed formulation were also compared to the results of the equations proposed by Cai *et al.* (2017) and Pain *et al.* (2017). As observed, the equations proposed by Cai *et al.* (2017) and Pain *et al.* (2017) predicted substantially large passive pressure near the base of the wall. There is no experimental measurement to verify the value of passive pressure at the wall base; however, the predicted values using Cai *et al.* (2017) and Pain *et al.* (2017) equations are considerably and unrealistically greater than the calculated values by the proposed equation in this study. Also, the equation of Pain *et al.* (2017) predicted non-zero pressure values at top of the wall which is not the case for non-surcharge condition.

Calculated passive pressures using the proposed equation is compared with measurements of Dou *et al.* (2017) in Fig. 5. As observed, there is a satisfactory good agreement between the results of experimental data and the proposed equation for all three relative densities of sand and the nonlinear distribution of passive earth pressure was correctly predicted using the proposed equation.

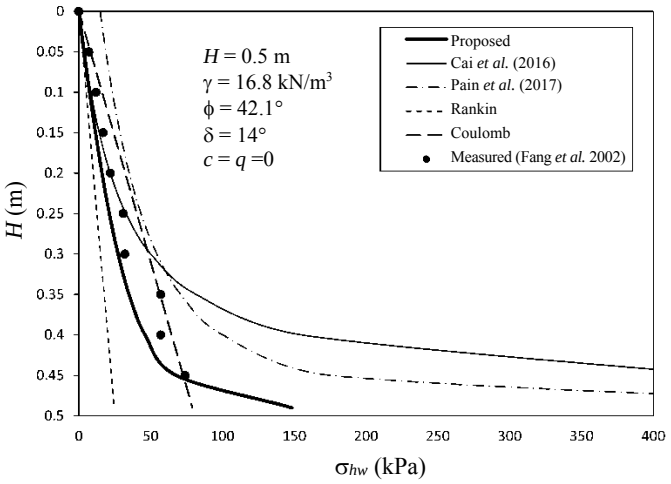

Fig. 4 Comparison of passive earth pressure by analytical equations and test results

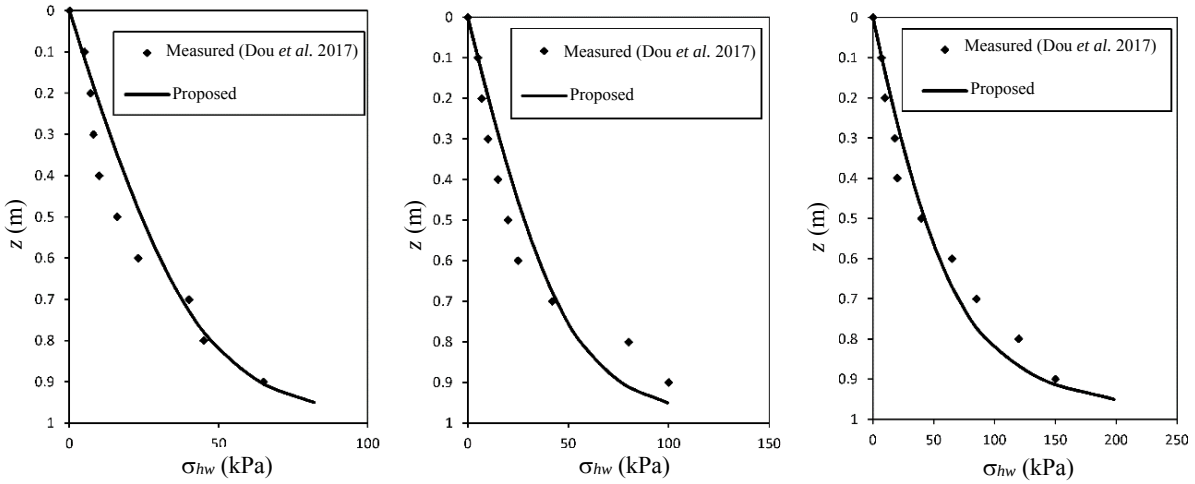

(a) Loose sand (b) Medium dense sand (c) Dense sand

Fig. 5 Comparison of passive earth pressure by proposed equation and test results of Dou *et al.* (2017)

3.2 Magnitude and Application Point of Passive Thrust

In Table 1, the total passive force and its height of application in different studies were compared for the Fang *et al.* (2002) experiment. As observed, the passive force and its height of application using the proposed equation, are in good agreement with the measured values. On the other hand, the Coulomb's equation predicts larger values for both passive force and its height of application than both the proposed equation and the measured values. As indicated, the predicted passive forces using Cai *et al.* (2017) and Pain *et al.* (2017) equations are considerably greater than the Coulomb's equation.

Figure 6 is presented for comparison of the results of passive force and the height of application from this study with experimental result of Dou *et al.* (2017). The calculated values using the formulations of Coulomb's (1776); Rankine (1857); Cai *et al.* (2017) and Pain *et al.* (2017) were also plotted on this figure. As observed, there is superb agreement between the results of experimental data and the proposed equation. For this experiment, the equation of Pain *et al.* (2017) gives satisfactory values for passive thrust, however, its prediction for height of application is poor. Vice versa, the height of application was reasonably calculated by equation of Cai *et al.* (2017), but, the calculated passive thrusts are higher than the measured values.

Table 1 Comparison of passive force and its height of application by analytical equations and test results

	Passive force (kN/m)	Height of application (m)
Fang *et al.* (2002)	17.6	0.153
Cai *et al.* (2016)	49.9	0.093
Pain *et al.* (2017)*	29.2	0.162
Coulomb	20.2	0.167
Rankine	10.6	0.167
Current study	16.5	0.118

* Because of the extraordinary large values at the wall base, the calculations were done for 95% of the wall height.

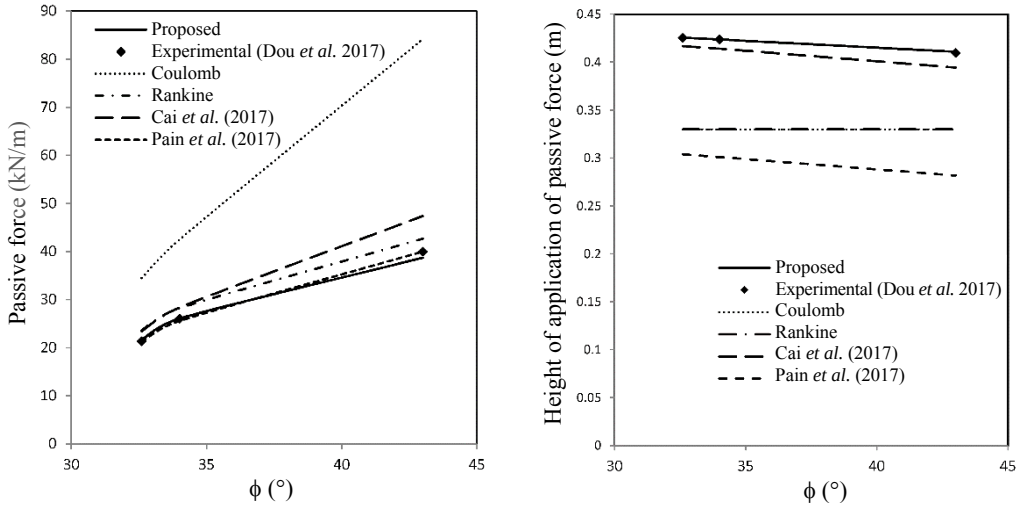

(a) Passive thrust (b) Height of application

Fig. 6 Comparison of passive thrust and height of application by proposed equation and test results of Dou *et al.* (2017)

4. PARAMETRIC ANALYSIS

This section discusses the effect of various parameters on the passive pressure distribution on a rigid retaining wall. These parameters include the internal friction angle (ϕ), cohesion I, and unit weight (γ) of backfill soil, surcharge pressure (q) on the backfill, soil-wall friction angle (δ), and height (H) of the retaining wall.

4.1 Internal Friction Angle of Backfill Soil (ϕ)

Figure 7 shows the effect of internal friction angle of backfill soil on the lateral passive pressure distribution for a 10 m high retaining wall. The soil parameters were considered γ = 19 kN/m^3, c = 10 kPa, q = 10 kPa, and δ = 0.8 ϕ. Friction angles from 15° to 35° were used in this graph. As observed, increasing the internal friction angle of the soil significantly increased the passive pressure. The effect of friction angle on the passive pressure increases by depth and the passive pressure at the wall base is considerably affected by the friction angle.

4.2 Cohesion of Backfill Soil I

The effect of soil cohesion can be seen in Fig. 8. The wall and soil parameters were considered H = 10 m, γ = 19 kN/m^3, ϕ = 30°, δ = 24°, and q = 20 kPa. Soil cohesion values from 5 to 20 kPa were used. As observed, an increase in soil cohesion slightly increased the passive pressure. Comparing to the Coulomb's method, the increasing effect of soil cohesion on passive pressure is negligible in the proposed formulation.

4.3 Unit Weight of Backfill Soil (γ)

The effect of unit weight of backfill soil is presented in Fig. 9. The wall and soil parameters were considered H = 10 m, c = 10 kPa, ϕ = 30°, δ = 24°, and q = 20 kPa. The passive soil pressure distribution was plotted for unit weights of 17 to 21 kN/m^3. As observed, an increase in the unit weight of the backfill soil increased the passive pressure.

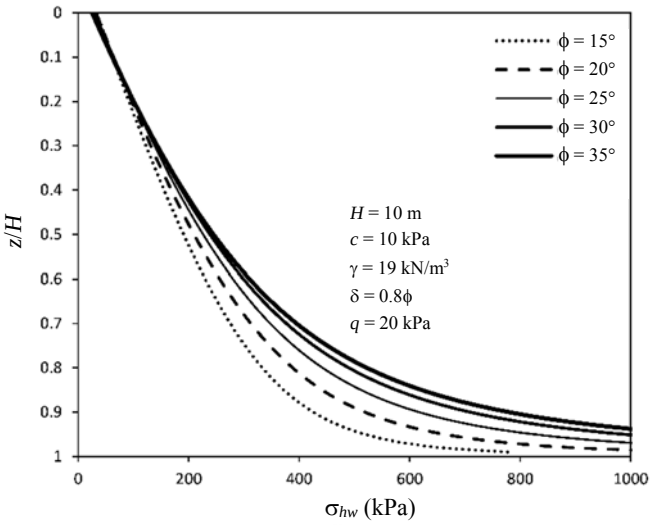

Fig. 7 Effect of internal friction angle of backfill soil on lateral passive pressure

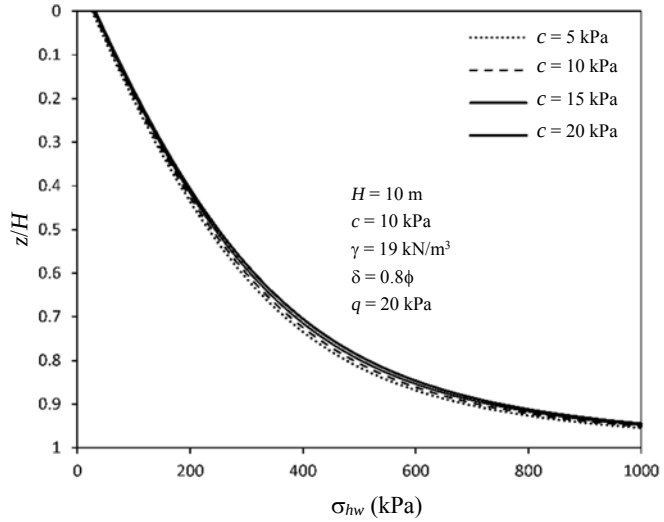

Fig. 8 Effect of cohesion of backfill soil on lateral passive pressure

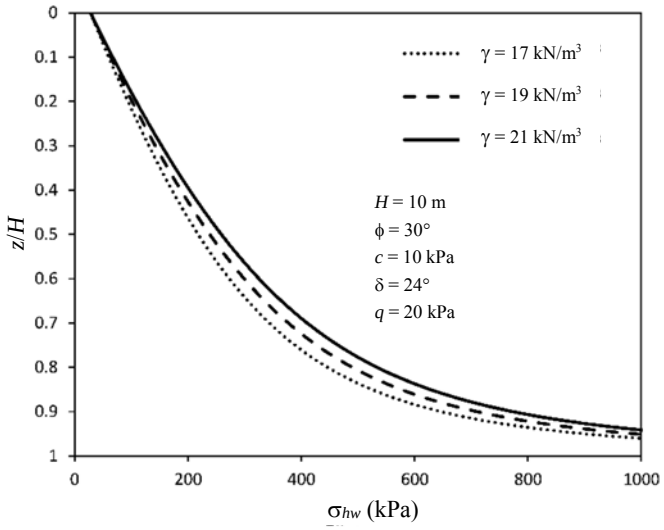

Fig. 9 Effect of unit weight of backfill soil on lateral passive pressure

4.4 Surcharge Pressure (q)

The effect of surcharge pressure on the backfill soil is presented in Fig. 10. The wall and soil parameters were considered H = 10 m, c = 10 kPa, ϕ = 30°, γ = 19 kN/m^3 and δ = 24°. The lateral passive pressure distribution for surcharge pressures of 10 to 40 kPa was plotted in Fig. 10. As observed, an increase in the surcharge increased the passive pressure. Note that as the surcharge increased, the passive pressure diagrams shifted parallel to each other toward the positive values. Comparing to the Coulomb's method, the increasing effect of surcharge on passive pressure is smaller in the proposed formulation.

4.5 Soil-Wall Friction Angle (δ)

The effect of soil-wall friction angle is presented in Fig. 11. The wall and soil parameters were considered H = 10 m, c = 10

kPa, ϕ = 30°, γ = 19 kN/m^3, and q = 20 kPa. The passive pressure distribution for soil-wall friction angles of 0°, 5°, 10°, 15°, 20° were plotted in this figure. As seen, an increase in δ decreased the magnitude of passive pressure on the upper zone of the wall height, as opposed to the lower zone of the wall height. For minor soil-wall friction angles, the distribution of passive pressure is nearly triangular and equal to the Rankine equation.

It is notable that the soil-wall friction angle plays an important role in the Coulomb's passive equation. For example, using the above parameters, the Coulomb's passive pressure coefficient varies from 3.0 to 6.1, *i.e.*, it increases about two times. However, the effect of soil-wall friction angle in the proposed equation is mainly on the distribution of passive pressure and its effect on the value of passive thrust is not as much as that of the Coulomb's equation.

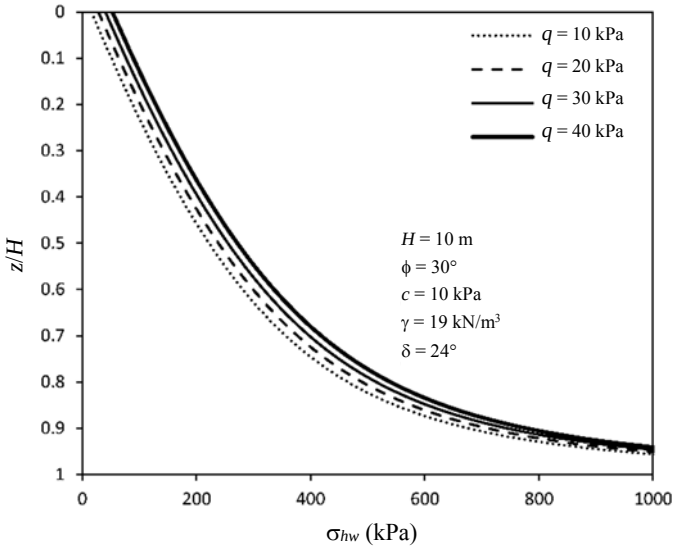

Fig. 10 Effect of surcharge pressure on lateral passive pressure

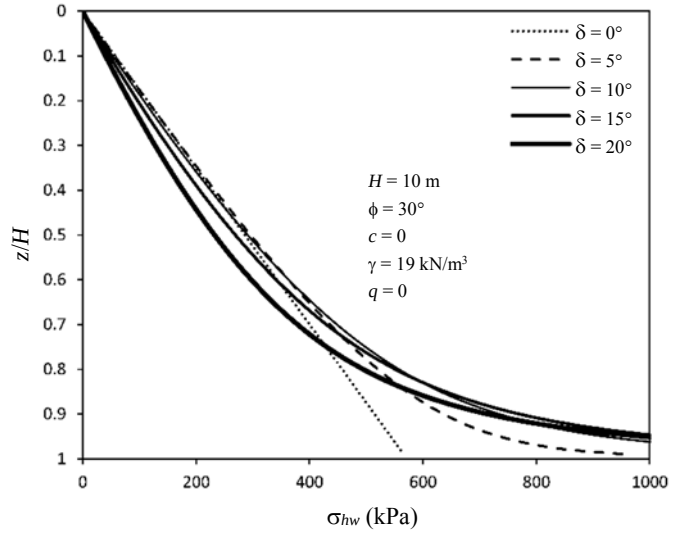

Fig. 11 Effect of soil-wall friction angle on lateral passive pressure

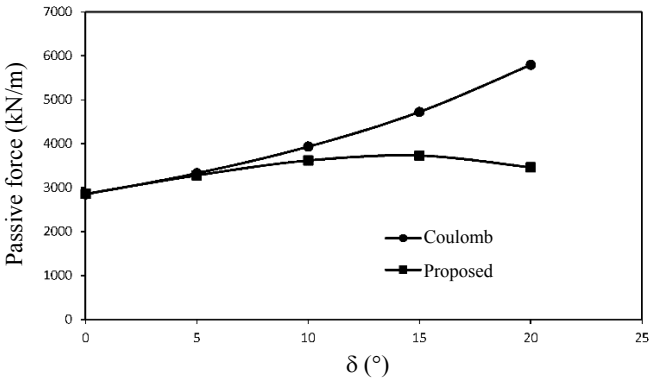

Fig. 12 Comparison of the effect of soil-wall friction angle on passive force between proposed and Coulomb's equations

Variation of passive force with soil-wall friction angle is presented in Fig. 12 for Coulomb's and propose equations. It can be observed that using Coulomb's equation, passive force increases by two times as the soil-wall friction angle increases from 0° to 20°, however, its effect in the formulation of this study is about 20% increase.

4.6 Wall height (*H*)

The effect of wall height is presented in Fig. 13. The soil parameters were considered c = 10 kPa, ϕ = 30°, γ = 19 kN/m^3, δ = 24° and q = 20 kPa. The passive pressure distribution for wall heights of 4 to 10 m was plotted in this figure. As observed, increasing the wall height significantly increased the passive pressure.

In Table 2, the results of proposed equation for passive force and its height of application are compared with Coulomb's equation, considering a wall with 10 m height and various combinations of soil parameters. The results are plotted in Figs. 14(a) and 14(b). As observed, using the proposed equation, the calculated values for passive force and its height of application point are lesser than Coulomb's equation.

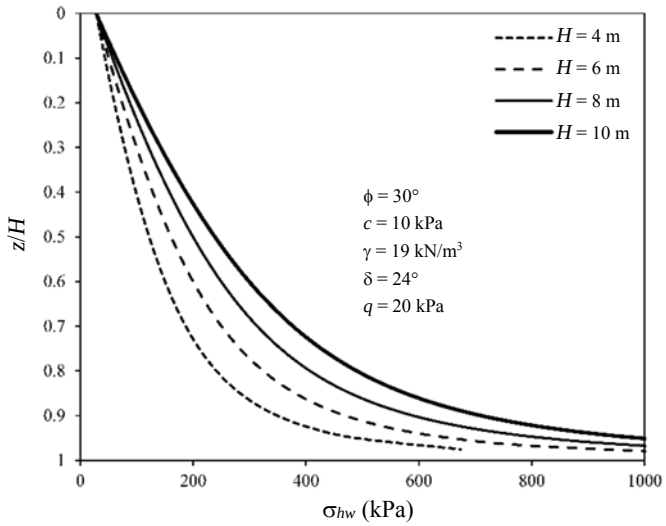

Fig. 13 Effect of wall height on lateral passive pressure

Table 2 Comparison of the proposed model results with Coulomb's equation

Soil parameters			Passive force (kN/m)		Height of application (m)	
c (kPa)	ϕ (°)	δ (°)	Proposed	Coulomb's	Proposed	Coulomb's
0	15	0	1614	1597	3.33	3.33
0	15	8	1797	1913	3.02	3.33
0	15	12	1717	2101	2.90	3.33
0	15	15	1321	2260	2.92	3.33
0	25	12.5	2884	3340	2.74	3.33
0	25	20	2491	4322	2.55	3.33
0	35	18	4879	7085	2.32	3.33
0	35	28	3291	12487	2.25	3.33
5	15	8	1945	2055	3.10	3.53
5	15	12	1830	2249	2.93	3.53
5	25	12.5	3066	3528	2.79	3.50
5	25	20	2601	4535	2.56	3.49
5	35	18	5093	7358	2.35	3.48
5	35	28	3381	12850	2.25	3.46
10	15	8	2093	2197	3.16	3.63
10	15	12	1943	2398	2.95	3.62
10	25	12.5	3248	3715	2.84	3.58
10	25	20	2712	4749	2.57	3.57
10	35	18	5308	7631	2.38	3.54
10	35	28	3470	13212	2.24	3.51

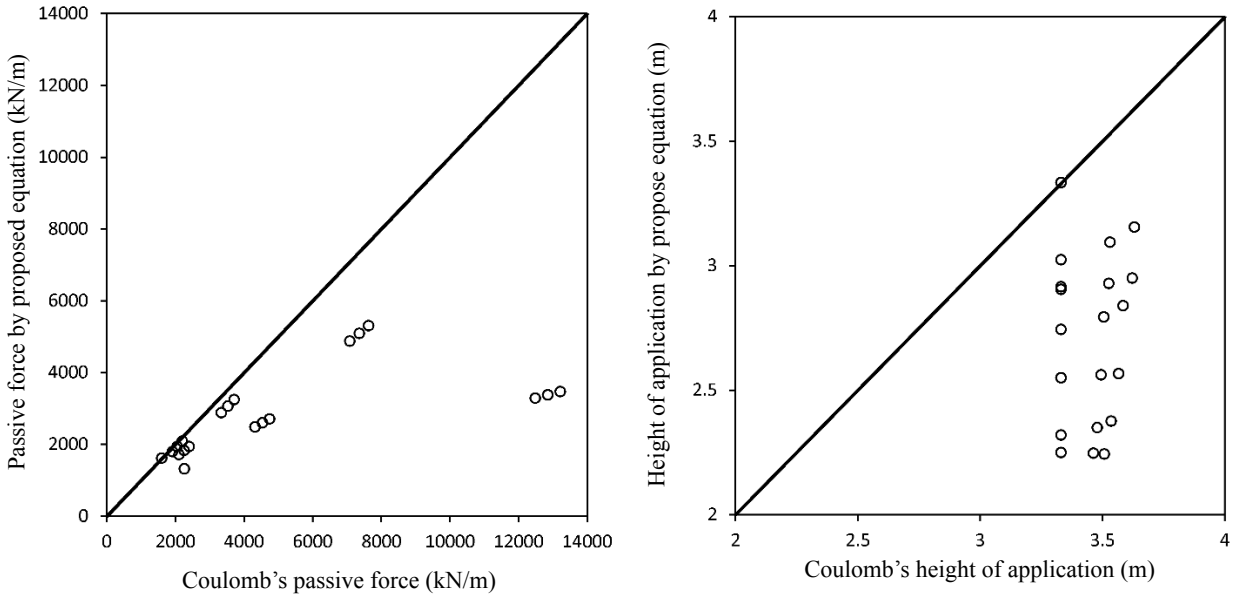

(a) Passive force (b) Height of application point

Fig. 14 Comparison of proposed equation and Coulomb's equation

5. CONCLUSIONS

In this study, a comprehensive equation for passive earth pressure was developed using the principal stress rotation assumption. In the proposed equation, the shortcomings of the previous studies were modified in such a way that it works well in all ranges of parameters. The results of the proposed equation indicate that the soil-wall friction produces major changes in the distribution of passive earth pressure and make it nonlinear in the height of the wall. Both of the passive thrust and its height of application were predicted smaller than the Coulomb's equation. Also, the increasing effect of soil cohesion and surcharge on passive pressure was obtained significantly less than the Coulomb's method. Therefore, using the Coulomb's passive equation for checking of sliding and overturning of retaining walls is not in the safe side.

REFERENCES

Cai, Y., Chen, Q., Zhou, Y., Nimbalkar, S., and Yu, J. (2017). "Estimation of passive earth pressure against rigid retaining wall considering arching effect in cohesive-frictional backfill under translation mode." *International Journal of Geomechanics,* ASCE, **17**(4), 04016093. https://doi.org/10.1061/(ASCE)GM.1943-5622.0000786

Coulomb, C.A. (1776). "Essai sur une application des règles des maximis et minimis à quelques problèmes de statique relatifs à l'architecture." *Mèm Acad. Roy. Près. Divers Savants* 7, Paris (in French).

Dou, G., Xia, J., Yu, W., Yuan, F., and Bia, W. (2017). "Non-limit passive soil pressure on rigid retaining walls." *International Journal of Mining Science and Technology*, **27**(3), 581-587. https://doi.org/10.1016/j.ijmst.2017.03.020

Fang, Y.S. and Ishibashi, I. (1986). "Static earth pressures with various wall movements." *Journal of Geotechnical Engineering,* ASCE, **112**(3), 317-333. https://doi.org/10.1061/(ASCE)0733-9410(1986)112:3(317)

Fang, Y.S., Chen, T.J., and Wu, B.F. (1994). "Passive earth pressures with various wall movements." *Journal of Geotechnical Engineering,* ASCE, **120**(8), 1307-1323. https://doi.org/10.1061/(ASCE)0733-9410(1994)120:8(1307)

Fang, Y.S., Ho, Y.C., and Chen, T.J. (2002). "Passive earth pressure with critical state concept." *Journal of Geotechnical Engineering,* ASCE, **128**(8), 651-659. https://doi.org/10.1061/(ASCE)1090-0241(2002)128:8(651)

Goel, S., and Patra, N. (2008). "Effect of arching on active earth pressure for rigid retaining walls considering translation mode." *International Journal of Geomechanics,* ASCE, **8**(2), 123-133. https://doi.org/10.1061/(ASCE)1532-3641(2008)8:2(123)

Handy, R.L. (1985). "The arch in soil arching." *Journal of Geotechnical Engineering,* ASCE, **111**(3), 302-318. https://doi.org/10.1061/(ASCE)0733-9410(1985)111:3(302)

Harrop-Williams, K. (1989). "Arch in soil arching." *Journal of Geotechnical Engineering,* ASCE, **115**(9), 415-419. https://doi.org/10.1061/(ASCE)0733-9410(1989)115:3(415)

James, R.G. and Bransby, P.L. (1970). "Experimental and theoretical investigations of passive pressure problem." *Geotechnique*, **20**(1), 17-37. https://doi.org/10.1680/geot.1970.20.1.17

Khosravi, M.H., Pipatpongsa, T., and Takemura, J. (2016). "Theoretical analysis of earth pressure against rigid retaining walls under translation mode." *Soils and Foundations,* **56**(4), 664-675. https://doi.org/10.1016/j.sandf.2016.07.007

Li, J. and Wang, M. (2014). "Simplified method for calculating active earth pressure on rigid retaining walls considering the arching effect under translational mode." *International Journal of Geomechanics*, ASCE, **14**(2), 282-290. https://doi.org/10.1061/(ASCE)GM.1943-5622.0000313

Paik, K.H. and Salgado, R. (2003). "Estimation of active earth pressure against rigid retaining walls considering arching effects." *Geotechnique*, **53**(7), 643-653. https://doi.org/10.1680/geot.2003.53.7.643

Pain, A., Chen, Q., Nimbalkar, S., and Zhou, Y. (2017). "Evaluation of seismic passive earth pressure of inclined rigid retaining wall considering soil arching effect." *Soil Dynamics and Earthquake Engineering,* **100**, 286-295. https://doi.org/10.1016/j.soildyn.2017.06.011

Poncelet, J.V. (1840). "Mémoire sur la stabilité des revêtements et de leurs fondations." Note additionelle sur les relations analytiques qui lient entre elles la poussée et la butée de la terre. Mémorial de l'offi cier du génie, **13**.

Rankine, W.J.M. (1857). "On the stability of loose earth." *Philos Trans R Soc London*, **147**, 9-27. https://doi.org/10.1098/rstl.1857.0003

Rao, P.P., Chen, Q.S., Zhou, Y.T., Nimbalkar, S., and Chiaro, G. (2016). "Determination of active earth pressure on rigid retaining wall considering arching effect in cohesive backfill soil." *International Journal of Geomechanics,* ASCE, **16**(3), 04015082. https://doi.org/10.1061/(ASCE)GM.1943-5622.0000589

Rowe, P.W. and Peaker, K. (1965). "Passive earth pressure measurements." *Geotechnique*, **15**(1), 57-78. https://doi.org/10.1680/geot.1965.15.1.57

Tang, Z.C. (1988). "A rigid retaining wall centrifuge model test of cohesive soil." *Journal of Chongqing Jiaotong University*, **25**(2), 48-56.

Tsagareli, Z.V. (1965). "Experimental investigation of the pressure of a loose medium on retaining wall with vertical back face and horizontal backfill surface." *Soil Mechanics and Foundation Engineering,* ASCE, **91**(4), 197-200. https://doi.org/10.1007/BF01706095

Xie, Y. and Leshchinsky, B. (2016). "Active earth pressures from a log-spiral slip surface with arching effect." *Géotechique Letters*, **6**(2), 149-155. https://doi.org/10.1680/jgele.16.00015

Zhou, Y., Chen, Q., Chen, F., Xue, X., and Basack, S. (2016). "Active earth pressure on translating rigid retaining structures considering soil arching effect." *European Journal of Environmental and Civil Engineering,* published online, 910-926. https://doi.org/10.1080/19648189.2016.1229225